Experimental Investigation of a Prandtl Probe Fabricated Using Desktop Stereolithography Technology

Alfred Gift Mwachugha, Jean Byiringiro, Harrison Ngetha, Thomas Carolus, and Kathrin Stahl

***Abstract* — A Prandtl probe is one of the standard instruments used for flow characterization in wind tunnel facilities. The convectional fabrication method of this instrument requires skilled artisanship, precision drilling, lathing and soldering of its several parts. This reflects into high costs of production in turn making wind energy studies expensive. With the adoption of additive manufacturing, the tooling costs, skills required and design to manufacture constraints can be addressed. This research presents a Prandtl probe that was designed using NX™ software, fabricated by desktop stereolithography additive manufacturing platform and validated in a wind tunnel for velocity range of 0 m/s to 51 m/s. This research attested the option of fabricating relatively cheap functional Prandtl probe with desktop stereolithography technology which can be used for accurate determination of flow quality in wind tunnels experiments. This provides various learning and research institution in developing countries that have already invested in additive desktop manufacturing technology certainty and a cheaper option to fabricate wind research instruments for use at their laboratories. Moreover, fabrication and validation of a 5-hole Prandtl probe can also be examined.**

***Index Terms*— Prandtl probe, stereolithography, wind tunnel, wind energy studies.**

I. INTRODUCTION

A. Overview

Research into renewable energy(RE) sources especially wind energy has rose over the last decade as a way to fulfil the ever increase in energy needs and countries devotion to reduce greenhouse gas emission globally [1]. In developing countries, most of the comprehensive research in RE technological developments is done in higher learning institutions [2]–[4]. Their laboratories are equipped with subsonic wind tunnels; with small test section, initially bought for conventional fluid dynamics undergraduate practicals [5]–[7]. With the interest into wind energy studies, these institutions are faced with the challenge of fitting their large test model at the test section. This presents a challenge whereby institutions opt either to design or buy new wind tunnels with bigger test sections or carry out their experiments at the exit end of these open jet subsonic wind tunnels. The latter being a cheaper option, a need to explore the quality of the exit flow such as the mean flow and velocity profile arises [8]. This is done using specialized wind speed measuring instruments such as the Prandtl probe.

The Prandtl probe was often used as a standard metrological instrument for flow speed measurements [9] and currently it is still being used as a tertiary standard [10]. This is because of its capability to give fast, accurate and reasonable repeatable measurements in a simple and inexpensive set up in a wind tunnel. Its first description was given by Henri Pitot in 1732 [11]. It is composed of two hollow tubes; one to measure the total pressure (Pt)[Pa], which has a port at the tip, directly facing the flow and the other one measures the static pressure (Ps)[Pa], which has a band of pressure ports downstream, parallel to the flow. From Bernoulli's principle, the difference of static pressure from the total pressure is the dynamic pressure, ΔP_{dyn}, from which the mean fluid velocity (with local air density calculated from atmospheric pressure and temperature measurements) is calculated using equation 1 and 2 [12], where ρ is the air density in [kg/m3].

$$\Delta P_{dyn} = P_t - P_s \tag{1}$$

$$U = \sqrt{\frac{2\Delta P}{\rho}} \tag{2}$$

The conventional fabrication method for the Prandtl probe requires skilled craftsmanship, precision drilling, lathing and soldering of its several parts. This leads to high cost of production in turn reflecting to high costs of wind energy studies. The emergence of desktop technology platform in additive manufacturing (AM)presents an opportunity to mitigate these high costs.

In the last decade, the three main pillars of AM; material, hardware and software have experienced tremendous growth. In materials, growth is seen in variety of materials ranging from metals, polymers and even ceramics. The hardware platform of today has faster, accurate and reliable systems while the current software makes the fabrication process streamlined and efficient. This has been made possible by the open-source community contribution and also the partnership between 3D printers and major material manufacturers [13], [14]. Furthermore, the layoffs seen during the conception of 3D printing has allowed all these three pillars and other futile applications to materialize. With all these advancement, the desktop 3D printer field is shifting from hobbyists fields to professional environments such as learning institutions and factories [15]–[18].

Published on October 30, 2020.
A. G. Mwachugha, Dedan Kimathi University of Technology, Kenya.
(e-mail: mwachugha.alfred16@students.dkut.ac.ke)
J. Byiringiro, Dedan Kimathi University of Technology, Kenya.
(e-mail: jean.bosco@dkut.ac.ke)
H. T. Ngetha, Dedan Kimathi University of Technology, Kenya.
(e-mail: harrison.ngetha@dkut.ac.ke)
T. Carolus, Institute of Fluid and Thermodynamic, Siegen University, Germany.
(e-mail:thomas.carolus@uni-siegen.de)
K. Stahl, Institute of Fluid and Thermodynamic, Siegen University, Germany.
(e-mail: kathrin.Stahl@uni-siegen.de)

At the professional environment, the desktop technology platforms are relatively cheap as they offer the opportunity to fabricate products at a fraction cost and footprint compared to industrial 3D printers [19]. In addition, this technology platform has the capability to manufacture intricate shaped structures with less waste, development and production time than conventional manufacturing technologies [20]. These advantages have already led it to be used in fabrication of instruments and equipment built for scientific research in fluid dynamics such as the liquid flow meters [21] and models for wind tunnel testing [22].

Therefore, the goal of this study is to investigate the capability of additive manufacturing desktop technologies, in particular desktop stereolithography(D_STL), to fabricate a functional Prandtl probe.

B. Current art

1) Wind tunnel

Since their commencement, their main application has been in affirming aerodynamics theories and in the design of airplanes. It is considered as a rapid and an accurate experimental tool in the field of fluid dynamics, which is mostly used to conduct aerodynamics research, validate numerical flow simulation and support design decisions [23]. Presently, research in aerodynamics has grown into other fields such as architectural, sports, environmental pollution and automotive hence creating the need for low speed wind tunnel (LSWT) tests rather than convectional large wind tunnels for research and design [24], [25].The test section of the most of these LSWT bought by many learning institutions in developing countries, are very small hence unable to fit the scaled models fabricated for research analysis. This presents a challenge whereby institutions opt either to design/buy new wind tunnels with bigger test sections or carry out their experiments at the exit end of these open jet subsonic wind tunnels. For the newly designed wind tunnels (being a cheaper option) and the option of carrying out experiments at the exit end of the existing open circuit wind tunnels, there is need to perform a number of flow characterization in order to explore the quality of the flow such as the mean flow, velocity profile, and turbulence /spectral intensity [8].

2) Wind Speed Measuring Instruments

In reference to the wind measurements technologies standard guidelines from EN 61400-12, ISO 17713-1 (2007) and ASTM D3796 [26] the various wind speed measuring instrument used at wind tunnels (ducts) for analyzing the flow uniformity and turbulence levels comprise of:

- Cup Anemometer
- Vane Anemometer
- Hot-wire Anemometer
- Pitot tube and Prandtl probe (Pitot - static tube)

From the instrument listed above, most of them measure the secondary wind effect and not the primary, that is, for example, in the cup anemometer, the cup rotates after the wind has blown over it, whereby the wind speed is calculated from the number of cup rotations per second. This introduces an error in the readings. With pressure anemometer such as the Prandtl probe, the dynamic pressure caused by wind is measured directly, thus wind speed readings are more accurate. In reference to this and their capability to give fast, accurate and reasonable repeatable measurements in a simple and inexpensive set up in a wind tunnel, they are recommended in EN61400-12-1 as standard instruments for wind tunnel calibrations and calibration of other anemometers [26].

3) Computational Fluid Dynamics (CFD)

CFD came into being during 1950s and early 1960s. It was prompt by the co-occurrence of high performance mainframe computers in relation to storage and execution as well as the essence of evaluating physical phenomena of high velocity and high temperatures [27], [28].

The second phase of CFD which is currently being used, is more of a descriptive discipline; it involves solving fluid dynamics problems with Navier Stoke governing equation (which are also more complicated) [28].

Currently, CFD is used to support and complement theory analysis and laboratory experiments as a third discipline in fluid dynamics. CFD has the advantage of providing detail flow field information that was formerly difficult to evaluate in wind tunnel tests [28], [29].

Works by Salter et al. [30] on the different types of nose shapes of Prandtl probe at a water tunnel, indicated that the modified ellipsoidal nose type had freedom of flow separation along the probe, hence a better alternative to both the tapered and hemispherical nose types. These results can be affirmed through enhanced flow field information in CFD simulations.

4) Additive Manufacturing (AM)

Over the last decade, there has been a shift where desktop 3D printers are finding their way in the professional environment as evident by the high number of purchases and growth in hardware, software and material in desktop 3D printers [31]. At the beginning, the AM arena was seen to be split into two: large scale manufacturing and concept modelers. The concept modelers field was made up of desktop 3D printers for office prototyping in the hobbyist domain while industrial/professional 3D printers dominated the factories floors [18]. Their penetration was made possible by expiring of major patents which resulted into markets for other manufacturers who are proposing new machines as well as by the contribution from open source community [32].

Furthermore, aside from being relatively cheap, desktop 3D printers offer the opportunity to fabricate products at a fraction cost and footprint compared to industrial 3D printers [33]. With these advancements, it provides an opportunity to test the maturity of this platform in the production of functional products similarly to industrial 3D printers.

II. Development of the Prandtl probe

A. Design of the Prandtl probe

In an overview, the Prandtl probe is comprised of the head and the stem. The head has two concentric tubes; affixed to a stem at right angle and extends to just one side (Fig. 1).

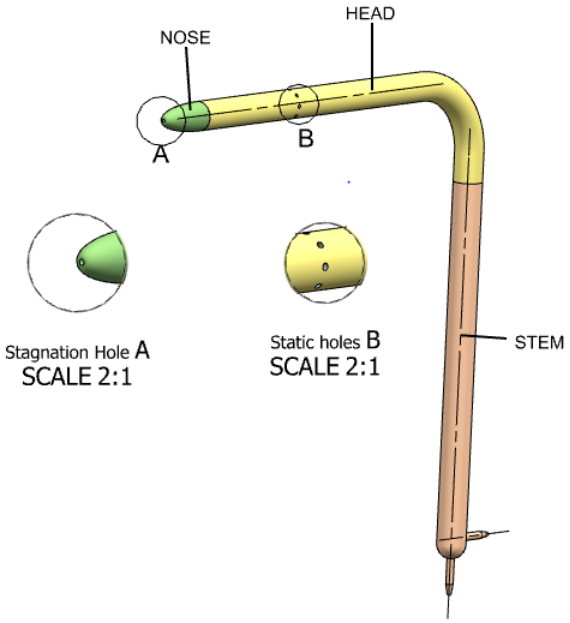

Fig. 1. Prandtl probe 3D drawing.

Design criterion of the nose (the upstream portion) is shaped in a special profile; modified ellipsoidal nose type. The tapered nose type and hemispherical nose type are both prone to flow separation along the tube which vary with Reynolds number and airstream turbulence. Fig. 2 (a) and (b) below show a 2D description and a CAD model of the proposed Prandtl probe respectively designed with the help of NX™ software. The diameter of the first prototype was 10mm.In order to find the smallest dimension that could be 3D printed, the probe diameter was reduced stepwise by 2mm.

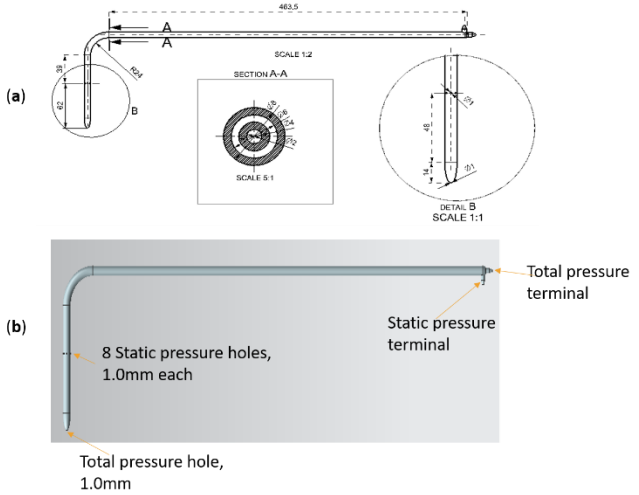

Fig. 2. (a) 2D description (b) CAD model of the proposed Prandtl probe.

B. Numerical investigation of flow separation in ellipsoidal nose profile

The analysis and visualization of flow around the nose shape was done with the help of ANSYS® FLUENT®, using the finite volume method.

Half of the nose body section was considered since the nose part is a symmetrical body. The axis parallel to the free stream velocity; the bottom boundary, was modelled as an axis boundary. The right boundary was modelled as pressure out flow while the left and top boundaries as velocity inlet. The ellipsoidal surface was considered to have properties of a wall. Furthermore, no-slip boundary condition was assumed to hold true for all solid-fluid interface, i.e. the ellipsoidal nose top surface. Fig. 3 depicts the boundary conditions and the mesh used.

The computational grid is sectioned into two areas: the free stream field and the boundary layer field. Meshing at the boundary layer area is refined and is attached to the ellipsoidal surface. There are more cells (mesh) at the ellipsoidal surface in order to compensate for the high velocity gradient in the boundary layer field of the free stream flow.

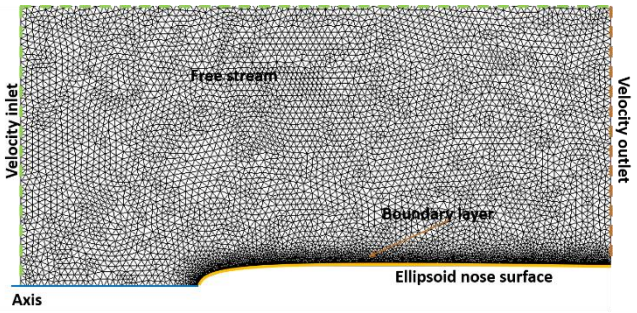

Fig. 3. Computational domain and boundary condition. Computational domain and boundary condition.

The two-dimensional modelling and steady state laminar pressure based simulation was conducted with the fluid defined as air and simulated at a constant inlet velocity of 1.5 m/s with turbulence intensity of 10%. Pressure outlet condition was set at 0 bar. k-w SST turbulence model was chosen for predicting accurate hydrokinetics flow and pressure gradients on the ellipsoidal nose surface. This model predicts accurately the onset and amount of flow separation in adverse pressure gradients, thus highly used in accurate boundary layer simulations. Convergence conditions for continuity and mass imbalances were set to less than 10^{-7} and simulation runs set to 1000 iterations. By comparison of different grid cell sizes, a grid independence study was achieved at cell count of 133,925, with any increase leading to no significant change in computational solution.

Fig. 4(a) below depicts the residual RMS error value having reduced to 10-8 while the domain imbalances being less than 1%. These satisfies the conditions for a steady state simulation solution. The skin friction coefficient distribution was used to locate points where the flow separates from the ellipsoidal nose surface, that is when skin friction coefficient value is zero. This is determined when the velocity gradient normal to the wall vanishes. Figure 4 below shows that no separation was observed from the ellipsoidal nose surface. This is further clearly visualized in the velocity contours around the ellipsoidal nose surface. The flow was observed to maintain its laminar state with zero velocity at solid-fluid interface (Fig. 4 (b) and (c) below). This affirmed the freedom of flow separation in modified ellipsoidal nose profile thus it was adopted during Prandtl probe design.

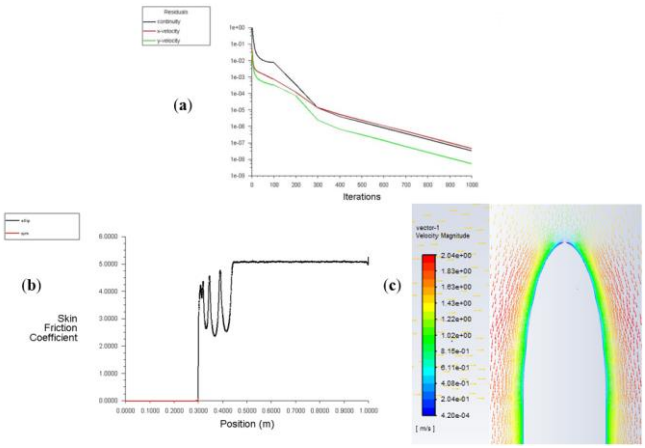

Fig. 4. CFD Analysis – (a) Computational mass and momentum imbalances, (b) Skin friction coefficient distribution at ellipsoidal nose surface and (c) Velocity contours around ellipsoidal nose surface.

C. Fabrication of Prandtl probe

Desktop stereolithography(D_STL) printer (Form 2^{TM}) from Formlabs company was used to perform the 3D printing task.

The printing process involved six steps (shown in Fig. 5 below).

- File exportation - The design was exported in. stl file format that's readable by the software Preform which prepares the file for the 3D printer (Form 2TM).
- Parameters setting - The printer parameters were adjusted in order to slice the imported. stl file into layer thickness that determined high output resolution for the 'prints'. More adjustable settings such as orientation, support structures, and material choice best for printing were set.
- Printing - A quick confirmation of the correct setup was performed automatically and then printing process began. The machine ran unattended until the printing process was complete. This included automatically refilling of the resin material from the cartridge tank.
- Cleaning - The printed parts were rinsed in isopropyl alcohol (IPA) to remove any uncured resin from their surface. In addition, air was also blown from the ends of the tube to remove any left resin or IPA.
- Curing - It involved the finalization of the polymerization process and stabilizing the mechanical properties. The printed parts were placed inside a curing chamber; advanced heating system of 13 multi-directional LED, for 1 hour at a 60 degree Celsius. This helped in finalizing polymerization process and stabilizing the 'print' mechanical properties.
- Finishing - The supports structures were removed using flush cutters and thereafter, the support marks left were removed through sanding by fine emery paper.

Fig. 5. Fabrication flow chart diagram.

Due to the limit of the printing platform in terms of height of the printer space, printing was composed of four parts. The printed parts were joined together using glue and tested for any leakages through blowing air in each pressure line in search of any leakages in form of air bubbles in a water pool and a pressure drop reading in a Betz manometer. No leakages were found by these inspection criterions.

A fully assembled fabricated Prandtl probe is shown in Fig. 6 below.

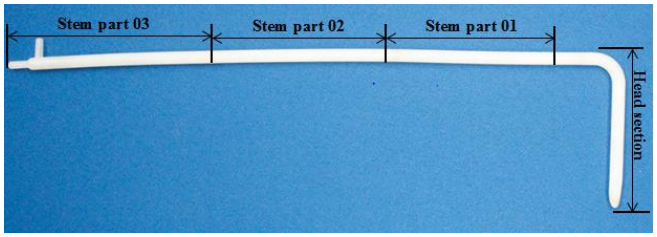

Fig. 6. Fully joined 3D printed Prandtl probe.

III. PRANDTL PROBE (PP) CALIBRATION AND VALIDATION

A. Preliminary tests

Two wind tunnels were used; wind tunnel 1 and 2. Spatial distribution of these wind tunnels were measured in order to determine the velocity profiles and turbulence properties of the air jets. Hot-wire of type TSI 1210-T1.5 was used as a measuring instrument. The measurement time per measurement point was set to 1 second with a sampling rate of 1000 Hz. The measured area for both wind tunnels was defined by x, y and z coordinate system (Fig. 7 and 8). The orientation of the Y-axis is parallel to the jet axis. A traverse (positioning) system was used to move the Hot-wire probe along the two spatial directions (x and z). Wind tunnel 1 area was 100 mm by 100 mm (nozzle cross-section plus 20 mm edge on each side). Wind tunnel 2 area was 420 mm by 420 mm (nozzle cross-section plus 10 mm edge on each side).

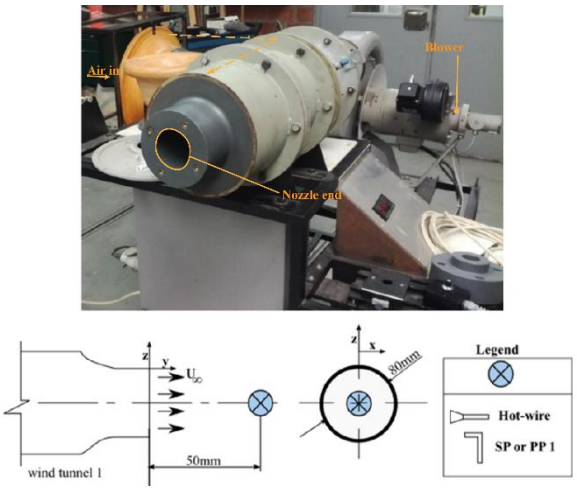

Fig. 7. Orientation at wind tunnel 1.

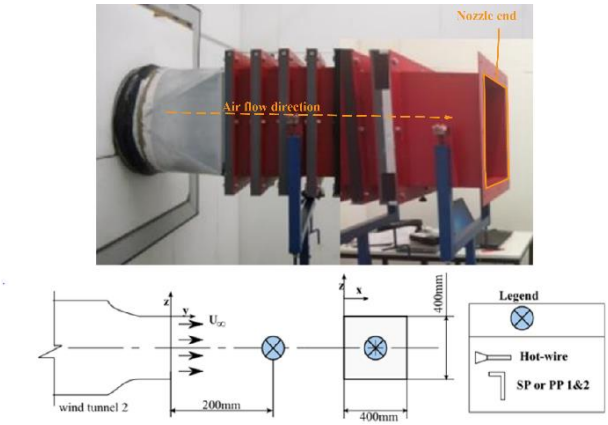

Fig. 8. Orientation at wind tunnel 2.

The velocity profiles (Fig. 9 below) for both wind tunnels are almost uniform at the center with decreasing velocity towards the edge. This is due to the fact that as the flow enters the free flow region it is mixed with the ambient air hence decreasing its velocity. The further the distance from the center of the nozzle along x and z axes; the higher the decrease in velocity.

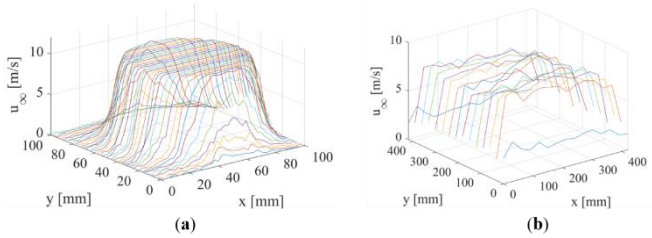

Fig. 9. Sample velocity profiles of wind tunnel 1(a) and 2 (b).

B. *Calibration*

Wind tunnel 1 was used as a source of air flow for velocity between 1 m/s to 48 m/s. PP 1 and PP 2 (having 10 mm and 8 mm diameter respectively) probe were calibrated using this rig against a standard (reference) metallic Prandtl probe (SP) probe as reference instrument.

Figure 10 below shows the calibration graphs of PP 1 probe at wind tunnel 1and 2. From these graphs, it is seen that, when PP 1 probe is used for velocity measurements it gives accurate measurement results similar to SP probe. PP 2 (having an 8 mm diameter) line of best fit is given as U = 1.0000 Upp2 - 0.0064 and U = 1.0061 Upp2 - 0.0314 (Fig. 10 a and b). This clearly shows that similar results can be obtained by PP 2 when used in place of SP.

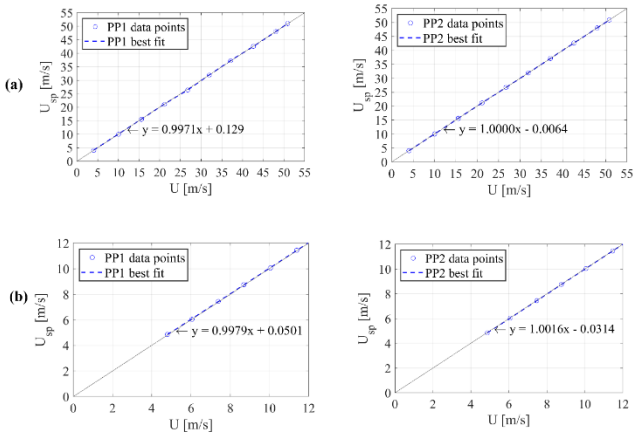

Fig. 10. Calibration graphs of PP 1 and PP 2 at; (a) wind tunnel 1 and (b).wind tunnel 2.

C. *Validation*

Wind tunnel 2 was used as source of air flow for velocity between 4 m/s to 13 m/s. Velocity readings of both the cup and hot-wire anemometers were taken in this rig and compared to those of PP 1 and PP 2 probes. The set-up used is similar to Fig. 7 and 8 and the data and command flow charts are as shown in Fig. 11.

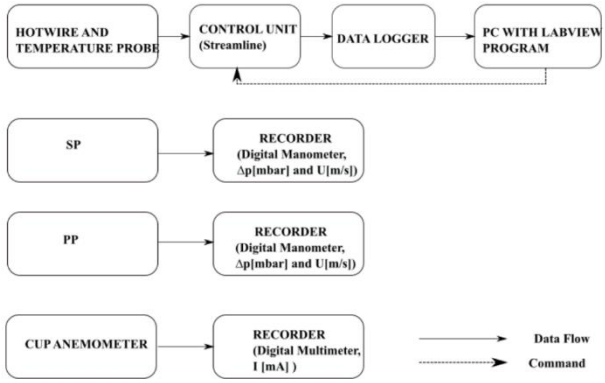

Fig. 11. Data and command flow diagrams.

Analysis in terms of comparison with other speed measuring instruments was done as shown in Fig. 12.

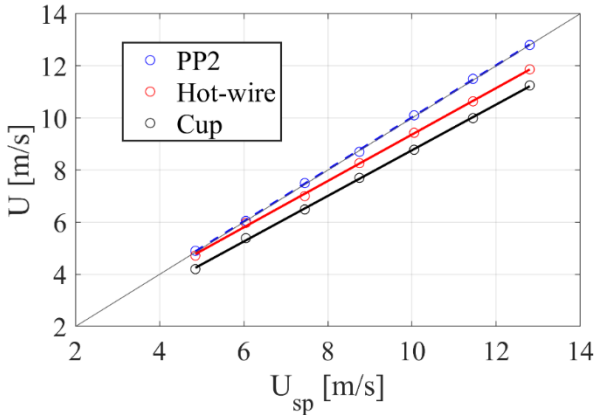

Fig. 12. Comparison with other wind measuring instruments - PP 2 against Cup and Hot-wire anemometers.

The cup and hot-wire anemometer velocity readings had small difference to the readings recorded by PP 2 as depicted in Fig. 12 above. These were accounted to temperature differences during calibration time and measurement sessions for hot-wire anemometer while for

cup anemometer it was due to the cup blockage effect. Minus these effects, the recorded velocity readings are similar to PP velocity readings hence demonstrate the capability of PP to give measurement results similar to both anemometers. This expresses the confidence of velocity measurements readings from a printed PP to be used in calibration of other flow measurement devices.

IV. Conclusion

The design, fabrication and experimental calibration and validation of rapid prototyped Prandtl probe are clearly demonstrated. NX™ software was used to produce the design. Stereolithography was the choice fabrication technique. A wind tunnel jet of range 0 to 51 m/s was used for the experimental investigation. A standard metallic Prandtl probe of 8 mm diameter in size, was used as the reference instrument. The printed Prandtl probes, cup and hot-wire anemometers were calibrated; then used to record velocity measurements. Velocity readings from the printed Prandtl probes were compared against those of cup and hot-wire anemometers.

The fabricated Prandtl probes, gave accurate velocity readings as evident from its velocity readings being similar as those of the reference instrument. Comparisons against cup and hot-wire anemometers showed small deviations in the anemometers readings which were due to temperature changes and cup blockage effect respectively.

This research showed it is possible to rapid prototype a Prandtl probe with a diameter of at least 8 mm which can be used for accurate velocity measurement in a wind tunnel jet. Furthermore, these findings indicate that desktop Stereolithography platform can produce Prandtl probes that are easier and cheap compared to complex and costly traditional convectional fabrication processes.

More validation of rapid prototyped Prandtl probes can be done, by testing the Prandtl probe in lower velocity below 4m/s in wind tunnel jets. For experiments carried out in high velocity and hot environments, a better choice of resin such as high temperature resin type which has a good structural stiffness from Formlabs company is recommended. In addition, fabrication and validation of a 5-hole Prandtl probe can also be examined with additive desktop platform techniques.

Appendix

TABLE I: Calibration Velocity Readings At Wind Tunnel 1

Wind source (rpm)	U_{spp} [m/s]		U_{ppp1} [m/s]		U_{ppp2} [m/s]	
	Run 1	Run 2	Run 1	Run 2	Run 1	Run 2
423	4.1	4	4	4	4	4.1
743	10.1	10	10	10	10	10.1
1055	15.6	15.6	15.6	15.4	15.6	15.6
1368	21.1	21.2	21.1	21.1	21.2	21.1
1678	26.5	27	26.5	26.3	26.8	26.7
1980	31.9	32	31.9	32	32	31.9
2276	37.1	37.1	37.2	37.3	37.2	37.1
2590	42.6	42.7	42.5	42.6	42.7	42.6
2900	48.1	48	48.1	48	48.1	48
3061	50.9	50.9	51	51	50.9	50.9

TABLE II: Velocity Readings At Wind Tunnel 2

Wind source [Hz]	U_{spp} [m/s]		U_{ppp1} [m/s]		U_{ppp2} [m/s]	
	Run 1	Run 2	Run 1	Run 2	Run 1	Run 2
20	4.8	4.9	4.7	4.9	4.8	4.9
25	6.1	6	6	6.1	6	6.1
30	7.4	7.5	7.3	7.5	7.4	7.5
35	8.8	8.7	8.6	8.8	8.7	8.8
40	10.1	10	10	10.1	10	10.1
45	11.4	11.5	11.3	11.5	11.4	11.5
50	12.8	12.8	12.8	12.8	12.8	12.8

TABLE III: Comparison Velocity Readings At Wind Tunnel 2

Wind source [Hz]	U_{ppp2} [m/s]		$U_{hotwire}$ [m/s]	$I_{cup\ anemometer}$ [m/s]	
	Run 1	Run 2		Run 1	Run 2
20	4.9	4.9	4.719	4.22	4.18
25	6	6.1	5.9717	5.37	5.42
30	7.5	7.5	7.0026	6.51	6.47
35	8.7	8.7	8.2651	7.7	7.71
40	10.1	10.1	9.4305	8.75	8.8
45	11.5	11.5	10.6372	9.98	9.99
50	12.8	12.8	11.8644	11.27	11.23

Acknowledgements

This work was carried out at Institute of Fluid and Thermodynamics laboratory, Siegen University, Germany in collaboration with Dedan Kimathi University of Technology, Kenya.

References

[1] Arndt C, Arent D, Hartley F, Merven B, Mondal AH. Faster Than You Think: Renewable Energy and Developing Countries. Annu. Rev. Resour. Econ. 2019;11(1):149–68.

[2] Davidsson H, Bernardo R, Gomes J, Gentile N, Gruffman C, Chea L et al. Construction of Laboratories for Solar Energy Research in Developing Countries. Energy Procedia 2014; 57:982–8.

[3] Clohessy, C. M., Brettenny, W., Sharp, G., & Vorster, F. Evaluation of noise levels of two micro-wind turbines using a randomised experiment. Journal of Energy in Southern Africa 2014;25(1):19-25.

[4] Akello, Philip Oketch, Francis Xavier Ochieng, andJoseph Ngugi Kamau. Performance analysis of a direct drive permanent magnet generator for small wind energy applications. Journal of Sustainable Research in Engineering 2016; 1:1–9.

[5] Selig, M., Deters, R., & Wiliamson, G. Wind Tunnel Testing Airfoils at Low Reynolds Numbers. American Institute of Aeronautics and Astronautics 2011.

[6] Eiduks, M., Viba, J., Shtals, L., Kovals, E., & Noskovs, S. Fluid flow vibration excitation by the control of interaction surface. Engineering for Rural Development (Lavitia) 2011:464–9.

[7] Jin-Jing, T. A. N., Myler, P., & Wen-An, T. A. N. Investigation and Analysis on Racing Car Front Wings. DEStech Transactions on Engineering and Technology Research 2016.

[8] Roberto A, Sausen G, M. A. Statistical Analysis of Wind Tunnel and Atmospheric Boundary Layer Turbulent Flows. Wind Tunnel Designs and Their Diverse Engineering Applications 2013 Mar 6:197–218.

[9] Vern E. Bean and J. Michael Hall. New Primary Standards for Air Speed Measurement at NIST. In Proceeding of the 1999 NCSL Workshop and Symposium Charlottle, NC. 1999, July.

[10] Shinder II, Crowley CJ, James Filla B, Moldover MR. Improvements to NIST'S air speed calibration service. Flow Measurement and Instrumentation 2015; 44:19–26.

[11] Brown GO. Henry Darcy's perfection ofthe Pitot tube. In Henry PG Darcy and Other Pioneers in Hydraulics 2003:14–23.

[12] E. Ower and R. C. Pankhurst. The Measurement of Air Flow, (1977). 5th ed.: Elsevier Ltd Pergamon Press; 1977.

[13] How Desktop 3D Printing is Moving From Makers to Pros. [June 22, 2020]; Available from: https://www.designnews.com/how-desktop-3d-printing-moving-makers-pros.

[14] Griffiths L. How desktop 3D printers became an essential industry tool. [March 04, 2020]; Available from: https://www.tctmagazine.com/additive-manufacturing-3d-printing-news/desktop-3d-printing-essential-industrial-tool/.

[15] Hardware, Materials and Software: the 3 Pillars of 3D Printing Success - AMFG. [April 04, 2020]; Available from: https://amfg.ai/2018/10/24/overcoming-3d-printing-challenges-3-pillars-of-success/.
[16] Thomas. The Evolution of 3D Printing. [April 04, 2020]; Available from: https://blog.thomasnet.com/evolution-of-3d-printing.
[17] Nichols G. Mass production 3D printing? It's coming, and it's a big deal. ZDNet 2019, 22 March 2019; Available from: https://www.zdnet.com/article/mass-production-3d-printing-its-coming-and-its-a-big-deal/. [April 04, 2020].
[18] Erin Winick. 3D printing's 30 year history and why it's popular now | by Erin Winick | Medium. [April 04, 2020].
[19] Formlabs Inc. 3D Printing Technology Comparison: FDM vs. SLA vs. SLS | Formlabs. [April 04, 2020].
[20] Thabiso Peter Mpofu, Cephas Mawere, Macdonald Mukosera. The Impact and Application of 3D Printing Technology 2014, June.
[21] Leigh, S. J., Purssell, C. P., Billson, D. R., & Hutchins, D. A. Using a magnetite/thermoplastic composite in 3D printing of direct replacements for commercially available flow sensors. Smart materials and structures. 2014;9(23).
[22] Olasek, K., & Wiklak, P. Application of 3D printing technology in aerodynamic study. Journal of Physics: Conference Series 2014, August;530.
[23] Tourn S, Pallarès J, Cuesta I, Paulsen US. Characterization of a new open jet wind tunnel to optimize and test vertical axis wind turbines. Journal of Renewable and Sustainable Energy 2017;9(3):33302.
[24] Gonzalez Hernandez MA, Moreno Lopez AI, A. A, Perales Perales JM, Wu Y, Xiaoxiao S. Design Methodology for a Quick and Low-Cost Wind Tunnel. " Wind tunnel designs and their diverse engineering applications." 2013(1).
[25] Ahmed N (ed.). Wind Tunnel Designs and Their Diverse Engineering Applications. 1st ed. Janeza Trdine 9, 51000 Rijeka, Croatia: InTech; 2013.
[26] J. Blackledge, B. Kearney, D. Kearney, K. O'Connell and B. Norton. Wind measurement technologies. Materials and processes for energy 2013.
[27] Blazek J. Computational Fluid Dynamics: Principles and Applications. 1st ed. Elsevier: Elsevier; 2001.
[28] Wendt JF. Computational fluid dynamics: an introduction.: Expository cartography for the humanities and social sciences. 3rd ed.: Springer Science & Business Media; 2008.
[29] Joel H. Ferziger, Milovan Peric. Computational Methods For Fluid Dynamics. 3rd ed. Verlag Berlin: Springer; 2001.
[30] Salter, C., Goodman, D. G., & Warsap, J. H. A Discussion of Pitot-static Tubes and of Their Calibration Factors with a Description If Various Versions of a New Design. National Physical Laboratory 1965.
[31] Kira. Wohlers Report 2016 reveals $1 billion growth in 3D printing industry. [April 04, 2020]; Available from: http://www.3ders.org/articles/20160405-wohlers-report-2016-reveals-1-billion-growth-in-3d-printing-industry.html.
[32] Gardan J. Additive manufacturing technologies: state of the art and trends. International Journal of Production Research 2016;54(10):3118–32.
[33] Formlabs Inc. 3D Printing Technology Comparison: FDM vs. SLA vs. SLS | Formlabs. [April 04, 2020].